

 Open access • Journal Article • DOI:10.1130/G25325A.1

Climate changes caused by degassing of sediments during the emplacement of large igneous provinces — [Source link](#)

Clément Ganino, Nicholas Arndt




Institutions: Joseph Fourier University

Published on: 01 Apr 2009 - Geology (Geological Society of America)

Topics: Large igneous province, Flood basalt, Siberian Traps, Extinction event and Volcano

Related papers:

- [Siberian gas venting and the end-Permian environmental crisis](#)
- [Large igneous provinces and mass extinctions](#)
- [On the ages of flood basalt events](#)
- [Release of methane from a volcanic basin as a mechanism for initial Eocene global warming](#)
- [Methane Release from Igneous Intrusion of Coal during Late Permian Extinction Events](#)

Share this paper:    

View more about this paper here: <https://typeset.io/papers/climate-changes-caused-by-degassing-of-sediments-during-the-14yly1y6ok>



HAL
open science

Climate changes caused by degassing of sediments during the emplacement of large igneous provinces

Clément Ganino, Nicholas Arndt

► **To cite this version:**

Clément Ganino, Nicholas Arndt. Climate changes caused by degassing of sediments during the emplacement of large igneous provinces. *Geology*, Geological Society of America, 2009, 37 (4), pp.323-326. 10.1130/G25325A.1 . hal-00371235

HAL Id: hal-00371235

<https://hal.archives-ouvertes.fr/hal-00371235>

Submitted on 27 Mar 2009

HAL is a multi-disciplinary open access archive for the deposit and dissemination of scientific research documents, whether they are published or not. The documents may come from teaching and research institutions in France or abroad, or from public or private research centers.

L'archive ouverte pluridisciplinaire **HAL**, est destinée au dépôt et à la diffusion de documents scientifiques de niveau recherche, publiés ou non, émanant des établissements d'enseignement et de recherche français ou étrangers, des laboratoires publics ou privés.

Climate changes caused by degassing of sediments during the emplacement of large igneous provinces

Clément Ganino and Nicholas T. Arndt

Laboratoire de Géodynamique des Chaînes Alpines, Université Joseph Fourier de Grenoble, CNRS, 1381 rue de la piscine 38400 Saint Martin d'Hères, France

Corresponding author: clement.ganino@ujf-grenoble.fr

Abstract

Most mass extinctions during the last 500 m.y. coincide with eruptions of large igneous provinces (LIP): the Cretaceous-Tertiary extinction was synchronous with the Deccan flood volcanism, Permian-Triassic extinction with the eruption of the enormous Siberian Traps, and End-Guadalupian extinction with the Emeishan volcanic province. The causal link remains disputed, however, and many LIPs apparently had no significant impact on the biosphere. Here we show that a key control on the destructive consequences of LIP emplacement is the type of sedimentary rock in basins beneath the flood basalts. Contact metamorphism around intrusions in dolomite, evaporite, coal or organic-rich shale generates large quantities of greenhouse and toxic gases (CO₂, CH₄, SO₂) which subsequently vent to the atmosphere and cause global warming and mass extinctions. The release of sediment-derived gases had a far greater impact on the environment than the emission of magmatic gases.

Keywords: large igneous province, mass extinction, contact metamorphism, sedimentary wall-rock, Emeishan

Introduction

During a mass extinction, taxa from a broad range of habitats and from throughout the world disappear within a geologically brief interval (~1Ma) (Hallam and Wignall, 1997). Vogt (1972) noted that the end-Cretaceous mass extinction was synchronous with eruption of the Deccan Traps flood basalts and Courtillot and Renne (2003) have catalogued many other coincidences between mass extinction and flood volcanism. In early papers the extinctions were attributed to poisoning (Vogt 1972), global warming (Jenkyns 1999) or global cooling (Budyko and Pivivariva, 1967; Axelrod, 1981) caused by the emission of volcanic gases. A problem with this interpretation is the absence of a good correlation between the volume of erupted basalt and the impact on the biosphere, as shown in Fig. 1. The eruption of the Siberian and Emeishan basalts coincide with major extinction but the Karoo basalts, for example, can be linked only to a period of global warming (McElwain et al., 1999). Nor does the latitude at the time of eruption, which influences the efficiency of atmospheric distribution of emitted gases and aerosols, correlate with the intensity of the environmental crisis.

Here we develop the ideas of Svensen et al. (2004, 2007) and Retallack and Jahren (2008) and propose that the intensity of global climate changes may be related to the type of rocks invaded by subvolcanic intrusive complexes, rather than to the volume or nature of the degassing lava. We present new data from contact aureoles surrounding intrusions of the Emeishan province in China, a province that coincides with the major

46 end-Guadalupian environmental crisis, and we link the environmental change to
47 massive release of CO₂ from the dolomites and organic-rich carbonates of the
48 underlying sedimentary basin. We contrast this setting with the more benign effects of
49 other LIPs which were emplaced upon older basalts, crystalline basement or
50 sedimentary rocks low in carbon and sulfur.
51

52 ***How do LIPs change the climate and cause mass extinctions?***

53 Major volcanic eruptions impact the environment in many ways: ash and sulphuric
54 acid aerosols lead to cooling, greenhouse gases like CO₂, CH₄ cause global warming;
55 SO₂ causes acid rain; F and other halogens poison plants and animals (see Thordarson
56 et al., 1996; Wignall, 2001 for a review). In all the LIPs shown in Figure 1, the
57 dominant magma is tholeiitic basalt which contains relatively low contents of magmatic
58 gases. Caldeira and Rampino (1990) estimated that the preruptive CO₂ concentration of
59 the Deccan magmas (~0.2 wt%) was sufficient to cause only modest global warming;
60 Self et al. (2006) confirmed that the mass of volcanic CO₂ was small compared with the
61 CO₂ already present in the atmosphere and they suggested that climate perturbations
62 were related to the emission of volcanic SO₂.

63 Many LIPs also contain minor alkalic magmas, volatile-rich magmas that may have
64 released larger quantities of volcanic gases, but there is little evidence that those
65 provinces with higher-than-normal alkali magma contents (e.g. Ethiopia) had a
66 disproportionate environmental impact (Courtilot and Renne, 2003). For reasons such
67 as these we explore the hypothesis that the killer mechanism that drives global warming
68 and mass extinctions is to be found in the sedimentary horizons beneath the flood
69 basalts.

70 ***A case study: sediment degassing during the emplacement of*** 71 ***the Emeishan LIP***

72 The current, post-erosional exposure the Emeishan LIP in SW China is relatively
73 small but the volcanic province may initially have covered >0.5 Mkm² (Courtilot and
74 Renne 2003). Its emplacement coincides with (1) a major sea-level fall (Hallam and
75 Wignall, 1999), (2) a negative ¹³C excursion (Retallack et al., 2006) and (3) the major
76 end-Guadalupian biological crisis when ~35% of all genera became extinct (Bowring et
77 al., 1998, Zhou et al., 2002). Magmas of the Emeishan LIP intruded Proterozoic to
78 Silurian dolostones, marls and shales of the Sichuan Basin.

79 Ganino et al. (2008) showed that the ~2000-m thick Panzhihua gabbroic sill, one of
80 many in the Emeishan province, developed a 300 m-thick contact aureole as it intruded
81 Proterozoic dolomites. The dominant rock type in the aureole is marble containing
82 about 30% brucite, the hydration product of periclase. The latter mineral formed during
83 prograde metamorphism of dolomite, a process that yields abundant CO₂. The trace
84 element composition of a brucite marble immediately adjacent to the intrusive contact
85 shows evidence of partial melting of carbonates; farther from the contact,
86 metamorphism of impure limestones formed calc-silicates. Both processes released
87 additional CO₂. Several hundred kilometres to the north-west of the Emeishan basalts,
88 shales and limestones of the Sichuan Basin contain gas and petroleum deposits (Wei et
89 al., 2008) and the metamorphism of hydrocarbons in contact aureoles may have
90 released CO₂ and CH₄. In the following section we quantify the amounts of CO₂
91 released from magmatic and sedimentary sources.
92

93 **Quantification of gas release during emplacement of the** 94 **Panzhihua intrusion**

95 Following Self et al.'s (2006) estimation of CO₂ release from Deccan volcanism,
96 we estimate that ~2 Gt of magmatic CO₂ (= 0.55 Gt C) was released from the 180 km³
97 of magma in the Panzhihua intrusion.

98 Three main reactions took place during the metamorphism of Panzhihua wall rocks,
99 depending on the temperature. We first focus on the intermediate-temperature
100 periclase-forming reaction dolomite = periclase + calcite + CO₂. From the reaction we
101 calculate that 240 g of CO₂ are released per kilogram of dolomite. From the dimensions
102 of the lower contact aureole (19 km long, 300 m wide and an assumed 3 km in depth),
103 we calculate its mass as ~ 47 Gt (density = 2700 kg.m⁻³) to give a total of 11.2 Gt of
104 CO₂ (or 3.1 Gt C). An equivalent mass of CO₂ probably was released by periclase
105 formation in an upper contact aureole, which is not preserved due to faulting.

106 We can use the presence of periclase, which formed at 700°C in samples collected
107 300 m from the intrusive contact, to define the temperature profile in the aureole (Fig.
108 2). We modelled the development of the aureole assuming that basaltic magma
109 continuously flowed through the sill to maintain a temperature of 1200°C at the contact.
110 In a simple conductive model, the profile requires 2500 years to form; when fluid
111 advection is taken into account, the time is shorter. Such a temperature profile explains
112 the presence of melted carbonates adjacent to the intrusion (~1200°C) and the presence
113 of periclase, which forms at ~700°C at a depth 300 m below the lower contact.

114 We now use this profile to estimate the quantities of gas released by high- and low-
115 temperature reactions (see supplementary material). The calculation is only
116 approximate because we have relatively little information about the exact geometry and
117 structure of the contact aureole, but it is sufficient to provide a first-order estimate.
118 High-temperature reactions such as the assimilation and partial melting of dolostone
119 yield abundant CO₂ but only within a few metres of the contact. An indication of the
120 amount of CO₂ that might be released by the assimilation of wall-rock in mafic magmas
121 is provided by Iacono Marziano et al. (2007) who calculated that lavas of Mt Vesuvius
122 had assimilated 15-17 wt% of limestone.

123 Calc-silicates form from impure marble between 450 and 500°C and these reactions
124 release between 220 and 290 g per kg of rock. Total degradation of hydrocarbons at
125 temperatures above 300°C would have released additional methane and CO₂. The large
126 range of concentration and maturation of organic carbon, preclude any precise
127 quantification of the mass of CO₂ released during low temperature degradation of
128 hydrocarbon, but some limits can be calculated. If the wall rocks contained a low
129 content of organic carbon (0.01 wt%) the input (0.02 Gt C) would be negligible but if
130 they contained 4 wt% organic carbon, as observed in source rock of the Sichuan Basin
131 (Wei et al., 2008), then the mass of CO₂ would be 8.1 Gt C, similar to that released
132 from the periclase reaction.

133 Given these results, we estimate that a total of at least 22 Gt of CO₂ from the
134 periclase reaction, and up to ~52 Gt equivalent CO₂ (=14.1 Gt C) if the wall-rock
135 contained large amount of organic carbon, was formed from the contact aureoles. These
136 values can be compared with the ~2 Gt CO₂ (=0.54 Gt C) released from the magma. At
137 the intrusion scale, the mass of sediment-derived carbon is some 11 to 26 times greater
138 than the mass of magmatic carbon.

139 **Gas-release during the Emeishan LIP at the basin scale**

140 Because of intense Himalaya-related deformation it is difficult to estimate the total
141 amount of sedimentary rock of the Sichuan Basin that was affected by metamorphism.
142 Taking as a model the better-preserved lava piles and sedimentary basins in the
143 Siberian and Karoo volcanic provinces (Czamanske et al., 2002; Chevallier and
144 Woodford, 1999), we assume that about half of the volume of the Emeishan volcanic
145 pile was emplaced as shallow-level intrusions. Courtillot and Renne (2002) calculate
146 that the total volume of the erupted basalt in the Emeishan LIP was $\sim 1 \text{ Mkm}^3$ and,
147 following Self et al.'s (2006) estimation for the Deccan, such a volume of magma
148 would release 11 200 Gt of CO_2 (= 3057 Gt C). Magma in intrusions emitted an
149 additional 5600 Gt of CO_2 bringing the total to 16800 Gt of CO_2 or 4585 Gt of C.

150 If the Panzihua intrusion is representative of an average sill in the intrusive
151 complex below the lava pile, 11 to 26 times more metamorphic CO_2 ($5600 \times 11 = 61600$
152 $5600 \times 26 = 145600$ Gt CO_2) was released from contact aureoles. Thus at the LIP scale,
153 the mass of sediment-derived CO_2 is about 3.6 to 8.6 times larger than the mass of
154 magmatic CO_2 .

155

156 **Proxies of climate change in Emeishan-age sediments**

157 Can CO_2 released during contact metamorphism of carbonates explain the negative
158 carbon isotope excursion at the end-Guadalupian which is recorded in both marine
159 carbonate and continental organic matter by Retallack et al. (2006)? During the end-
160 Guadalupian, the $\delta^{13}\text{C}$ of marine carbonates decreased from about +3 to -2 ‰, and that
161 of nonmarine clastic organic carbon from about -22 to -30 ‰ (Retallack et al., 2006). If
162 we suppose that 17000 Gt C from the destabilisation of dolostone (with $\delta^{13}\text{C} = 0$) and
163 22900 Gt C from the metamorphism of organic carbon (with $\delta^{13}\text{C} \sim -22$) were added to
164 the ocean-atmosphere, a global negative carbon isotope excursion would result (see
165 supplementary material for details). Atmospheric carbon composition would change
166 from $\delta^{13}\text{C} = -2$ before the degassing to as low as -10.9 after the degassing.

167 There are few reliable proxies for the climate changes during the emplacement of the
168 Emeishan LIP.

169 **Sediment degassing and mass extinctions**

170 Figure 2 is a synthesis of the total amount of volatiles released during the contact
171 metamorphism of different types of sedimentary rocks. The inputs that must be
172 considered when evaluating the environment impact of LIP emplacement can be
173 summarized as follows:

- 174 • Basalt and granitoids do not release abundant volatiles.
- 175 • In most sandstones, the main volatile is water whose release has little effect on
176 global climate.
- 177 • Pure limestone contains large amounts of CO_2 but the thermal decomposition of
178 limestone into CaO and CO_2 takes place at high temperatures ($>950^\circ\text{C}$) that are rarely
179 reached in contact aureoles.
- 180 • Impure limestones release large amounts of CO_2 (up to 29 wt%) during the
181 formation of calc-silicates at moderate temperatures of ~ 450 to 500°C .
- 182 • Gypsum and anhydrite in evaporites release abundant SO_2 (up to 47%). This
183 reaction normally happens at high temperatures (1400°C) that are not observed in
184 contact aureoles, but the reaction proceeds at temperature as low as 615°C for impure
185 anhydrite (West and Sutton, 1954).
- 186 • Contact metamorphism of salt releases halocarbons.

- 187 • Sulfidic sediments release abundant SO₂ at low temperature.
- 188 • Organic carbon-rich shales and carbonates release methane and hydrocarbon
- 189 when heated at relatively low temperature (<300°C).
- 190 • Coal releases abundant CO₂ if ignited.

191

192 Figure 1 shows that there is no clear link between volume of the LIP and magnitude of
193 mass extinction. Degassing of magmatic volatiles therefore cannot be the sole cause of
194 the environmental changes and mass extinctions and gas release from sediments may be
195 implicated in various ways:

196 1. The Ontong-Java oceanic plateau, the largest magmatic province, formed in a
197 submarine volcanic setting and is not associated with a large mass extinction. The
198 dominant wall rock is basalt which yields no toxic or greenhouse gases (dehydration of
199 altered basalt has little climatic impact). Eruption into water may have restricted release
200 of gas into the atmosphere.

201 2. Emplacement of the Deccan traps coincides with the K-T mass extinction (e.g.
202 Courtillot and Renne, 2002). Here the substrate consists of minor clastic sediments and
203 crystalline basement, which do not yield additional volatiles, and a combination of
204 Chixculub meteorite impact (e.g., Alvarez et al. 1980) and the release of magmatic
205 gases (Chenet et al., 2008) may account for the K-T mass extinction.

206 3. Eruption of the Siberian traps, the largest continental flood basalt province,
207 coincided with the largest known mass extinction. The volume of basalt cannot explain
208 the intensity of the crisis by itself. Intrusions beneath the Siberian traps invaded marls,
209 limestones, sandstones, coal and most significantly, evaporites (Czamanske et al.,
210 2002). The sulphur isotope signature of sulfide ores provides evidence that sulfur from
211 evaporites was assimilated into magma (Ripley et al., 2003). Part of the sulfur
212 contained in the magma was probably released as SO₂ during the eruption, and
213 additional SO₂, CO₂, the breakdown products of hydrocarbons, would be expelled from
214 the contact aureoles (Retallack and Jahren, 2008). Global dispersion of SO₂ from
215 Siberian traps volcanism was aided by the high latitude of these eruptions (e.g.,
216 Saunders, 2005).

217 4. The Emeishan plateau erupted at equatorial latitude and here the consequences
218 were different. The dispersion of CO₂ is largely independent of latitude because of the
219 high exchange rate between the stratosphere and the troposphere. We suggest therefore
220 that the coincidence between the Emeishan volcanism and the end-Guadalupian crisis
221 can be explained by the voluminous release of CO₂ from the heating of dolomite
222 augmented by CO₂, SO₂ and CH₄ from evaporites and shales.

223 In those provinces where the environmental impact was minor, the wall rocks were
224 sandstone, organic-poor shales or granitic basement. Svensen et al. (2007) estimated
225 that up to 27400 Gt may have formed during contact metamorphism of shales and
226 sandstones of the Karoo basin, enough to explain the Early Jurassic global warming but
227 not sufficient to cause a mass extinction. Likewise, the Central Atlantic Magmatic
228 Province coincides with the Triassic-Jurassic mass extinction but the influence of this
229 very large province may have been mitigated by the largely crystalline nature of its wall
230 rocks

231 **Conclusion**

232 Sedimentary rocks are huge reservoirs of volatiles that are readily released by contact
233 metamorphism. The degassing associated with contact metamorphism is much more
234 voluminous than the degassing of the magma itself. We have identified two major
235 mechanisms responsible for large gas emissions and mass extinctions: (1) the

236 destabilization of dolomite, which caused massive CO₂ release during the emplacement
237 of Emeishan and other LIPs, (2) the thermal decomposition of anhydrite, salt,
238 limestone, hydrocarbons and coal in other provinces, which provided a toxic cocktail
239 that caused other mass extinctions. Other provinces were emplaced in sterile magmatic
240 or sedimentary rocks and had little to no environmental impact.

241

242 **Acknowledgements**

243 We express our gratitude to Henrik Svensen for his constructive comments and his help
244 with the preparation of the manuscript. We also thank Catherine Chauvel, Fernando
245 Tornos, Lukas Baumgartner and Didier Marquer for constructive discussions; Mei-Fu
246 Zhou and Yuxiao Ma for assistance during our field work; and Chris Harris for
247 providing stable isotope analyses. The project was supported by two Egide exchange
248 programs PROCORE (France Hong Kong) and Aurora (France-Norway). Further
249 support was obtained from the French CNRS (DyETI program).

250

251 **References cited**

252 Alvarez, L.W., Alvarez, W., Asaro, F., and Michel, H.V., 1980. Extraterrestrial cause
253 for the Cretaceous Tertiary extinction: *Science*, v. 208, p. 1095–1108, doi:
254 10.1126/science.208.4448.1095.

255 Axelrod, D.I., 1981. Role of volcanism in climate and evolution: *Geol. Soc. Am., Spec.*
256 *Pap.* 185, 1–59.

257 Bowring, S.A., Erwin, D.H., Jin, Y.G., Martin, M.W., Davidek, K., and Wang W.,
258 1998, U/Pb Zircon Geochronology and Tempo of the End-Permian Mass
259 Extinction: *Science*, v. 280, p. 1039-1045, doi: 10.1126/science.280.5366.1039.

260 Budyko, M.I., and Pivivariva, Z.I., 1967, The influence of volcanic eruptions on solar
261 radiation incoming to the Earth's surface: *Meteorol Gidrol*, v. 10, p. 3–7.

262 Caldeira, K., and Rampino, M.R., (1990), Carbon dioxide emissions from Deccan
263 volcanism and a K/T boundary greenhouse effect: *Geophysical Research*
264 *Letters*, v. 17, p. 1299–1302.

265 Chenet, A.L., Fluteau, F., Courtillot, V., Gérard, M., and Subbarao, K.V., 2008,
266 Determination of rapid Deccan eruptions across the Cretaceous-Tertiary
267 boundary using paleomagnetic secular variation: Results from a 1200-m-thick
268 section in the Mahabaleshwar escarpment: *Journal of Geophysical Research*
269 v.113, B04101, doi: 10.1029/2006JB004635.

270 Chevallier, L., and Woodford, A., 1999, Morpho-tectonics and mechanism of
271 emplacement of the dolerite rings and sills of the western Karoo, South Africa:
272 *South African Journal of Geology*, v. 102, p. 43-54.

273 Courtillot, V., and Renne, P.R., 2003, On the ages of flood basalt events: *Comptes*
274 *Rendus Geoscience*, v. 335, p. 113-140, doi: 10.1016/S1631-0713(03)00006-3.

275 Czamanske, G.K., Zen'ko, T.E., Fedorenko, V.A., Calk, L.C., Budahn, J.R., Bullock,
276 J.H., Fries, T., King, B.-S., and Siems, D., 2002, Petrographic and geochemical
277 characterization of ore-bearing intrusions of the Noril'sk type. Siberia: With
278 discussion of their origin, including additional datasets and core logs: *US*
279 *Geological Survey Open-File Report*: 02-74.

280 Ganino, C., Arndt, N.T., Zhou, M.F., Gaillard, F., and Chauvel, C., 2008, Interaction of
281 magma with sedimentary wall rock and magnetite ore genesis in the Panzhihua
282 mafic intrusion, SW China, *Mineralium deposita*, 43, 677-694, doi:
283 10.1007/s00126-008-0191-5.

284 Hallam, A. and Wignall, P.G., 1997, Mass Extinctions and Their Aftermath: Oxford
285 University Press, 334 p.

286 Hallam, A. and Wignall, P.B., 1999, Mass extinctions and sea-level changes: Earth-
287 Science Reviews, v. 48, p. 217–250, doi: 10.1016/S0012-8252(99)00055-0.

288 Iacono Marziano, G., Gaillard, F., and Pichavant, M., 2007, Limestone assimilation by
289 basaltic magmas: an experimental re-assessment and application to Italian
290 volcanoes: Contributions to Mineralogy and Petrology, v. 154, p. 1-20, doi:
291 10.1007/s00410-007-0267-8.

292 Jenkyns, H.C., 1999, Mesozoic anoxic events and palaeoclimate: Zentralblatt für
293 Geologie und Paläontologie, p. 943–949.

294 McElwain, J.C., Beerling, D.J., and Woodward, F.I., 1999, Fossil Plants and Global
295 Warming at the Triassic-Jurassic Boundary: Science, v. 285, p. 1386-1390, doi:
296 10.1126/science.285.5432.1386.

297 Retallack, G.J., Metzger, C.A., Greaver, T., Jahren, A.H., Smith, R.M.H., and Sheldon,
298 N.D., 2006, Middle-Late Permian mass extinction on land: Bulletin of the
299 Geological Society of America, v. 118, p. 1398-1411, doi: 10.1130/B26011.1.

300 Retallack, G.J., and Jahren, A.H., 2008, Methane release from igneous intrusion of coal
301 during late Permian extinction events: The Journal of Geology, v. 116, p. 1-20,
302 doi: 10.1086/524120.

303 Ripley, E.M., Lightfoot, P.C., Li, C., and Elswick, E.R., 2003, Sulfur isotopic studies of
304 continental flood basalts in the Noril'sk region: implications for the association
305 between lavas and ore-bearing intrusions: Geochimica et Cosmochimica Acta,
306 v. 67, p. 2805-2817, doi:10.1016/S0016-7037(03)00102-9.

307 Rohde, R.A., and Muller, R.A., 2005, Cycles in fossil diversity: Nature v. 434, p. 208-
308 210, doi: 10.1038/nature03339.

309 Saunders, A.D., 2005, Large Igneous Provinces: Origin and Environmental
310 Consequences: Elements, v. 1, p. 259-263, doi: 10.2113/gselements.1.5.259.

311 Self, S., Widdowson, M., Thordarson, T., and Jay A.E., 2006, Volatile fluxes during
312 flood basalt eruptions and potential effects on the global environment: A Deccan
313 perspective: Earth and Planetary Science Letters, v. 248, p. 518-532,
314 doi:10.1016/j.epsl.2006.05.041.

315 Svensen, H., Planke, S., Malthe-Sørenssen, A., Jamtveit, B., Myklebust, R., Eidem, T.,
316 and Rey, S.S., 2004, Release of methane from a volcanic basin as a mechanism
317 for initial Eocene global warming: Nature, v. 429, p. 542-545, doi:
318 10.1038/nature02566.

319 Svensen, H., Planke, S., Chevallier, L., Malthe-Sørenssen, A., Corfu, B., and Jamtveit,
320 B., 2007, Hydrothermal venting of greenhouse gases triggering Early Jurassic
321 global warming: Earth and Planetary Science Letters, v. 256, p. 554-566, doi:
322 10.1016/j.epsl.2007.02.013.

323 Thordarson, T., Self, S., Óskarsson, N., and Hulsebosch, T., 1996, Sulfur, chlorine, and
324 fluorine degassing and atmospheric loading by the 1783-1784 AD Laki (Skaftár
325 Fires) eruption in Iceland: Bulletin of Volcanology, v. 58, p. 205-225,
326 doi:10.1007/s004450050136.

327 Vogt, P.R., 1972, Evidence for global synchronism in mantle plume convection, and
328 possible significance for geology: Nature, v. 240, p. 338-342, doi:
329 10.1038/240338a0.

330 Wei, G., Chen, G., Du, S., Zhang, L., and Yang, W., 2008, Petroleum systems of the
331 oldest gas field in China: Neoproterozoic gas pools in the Weiyuan gas field,
332 Sichuan Basin: Marine and Petroleum Geology, v. 25, p. 371-386, doi:
333 10.1016/j.marpetgeo.2008.01.009.

- 334 West, R.R. and Sutton W.J., 1954, Thermography of Gypsum: Trans. Central Geol.
335 Prospecting Znst (USSK), v. 88, p. 1-66.
- 336 Wignall, P.B., 2001, Large igneous provinces and mass extinctions: Earth-Science
337 Reviews, v. 53, p. 1–33, doi: 10.1016/S0012-8252(00)00037-4.
- 338 Zhou, M.-F., Malpas, J., Song, X.-Y., Robinson, P.T., Sun, M., Kennedy, A.K., Lesher,
339 C.M., and Keays, R.R., 2002, A temporal link between the Emeishan large
340 igneous province (SW China) and the end-Guadalupian mass extinction: Earth
341 and Planetary Science Letters, v. 196, p. 113-122, doi: 10.1016/S0012-
342 821X(01)00608-2.
- 343
- 344

345 Figure captions

346

347 **Fig 1. Volume of erupted basalt from Courtillot and Renne (2003) vs percentage of**
348 **generic extinctions (from *Rhodes and Muller 2005*) for major LIPs. Two main**
349 **populations of LIPs are evident, one for which the associated rate of extinction is**
350 **close to the background rate (Columbia River to Ontong Java) and another for**
351 **which the rate is far higher. Those in the latter group intrude sedimentary rocks**
352 **that released abundant greenhouse or toxic gases.**

353

354

355 **Fig 2. Theoretical thermal profile in a Panzhihua-like contact aureole. The**
356 **horizontal bars indicate the maximum distance into the aureole where the**
357 **metamorphic reactions take place. The black portion of each bar represents the**
358 **proportion of gas released by the reaction.**

359

360

Fig. 1

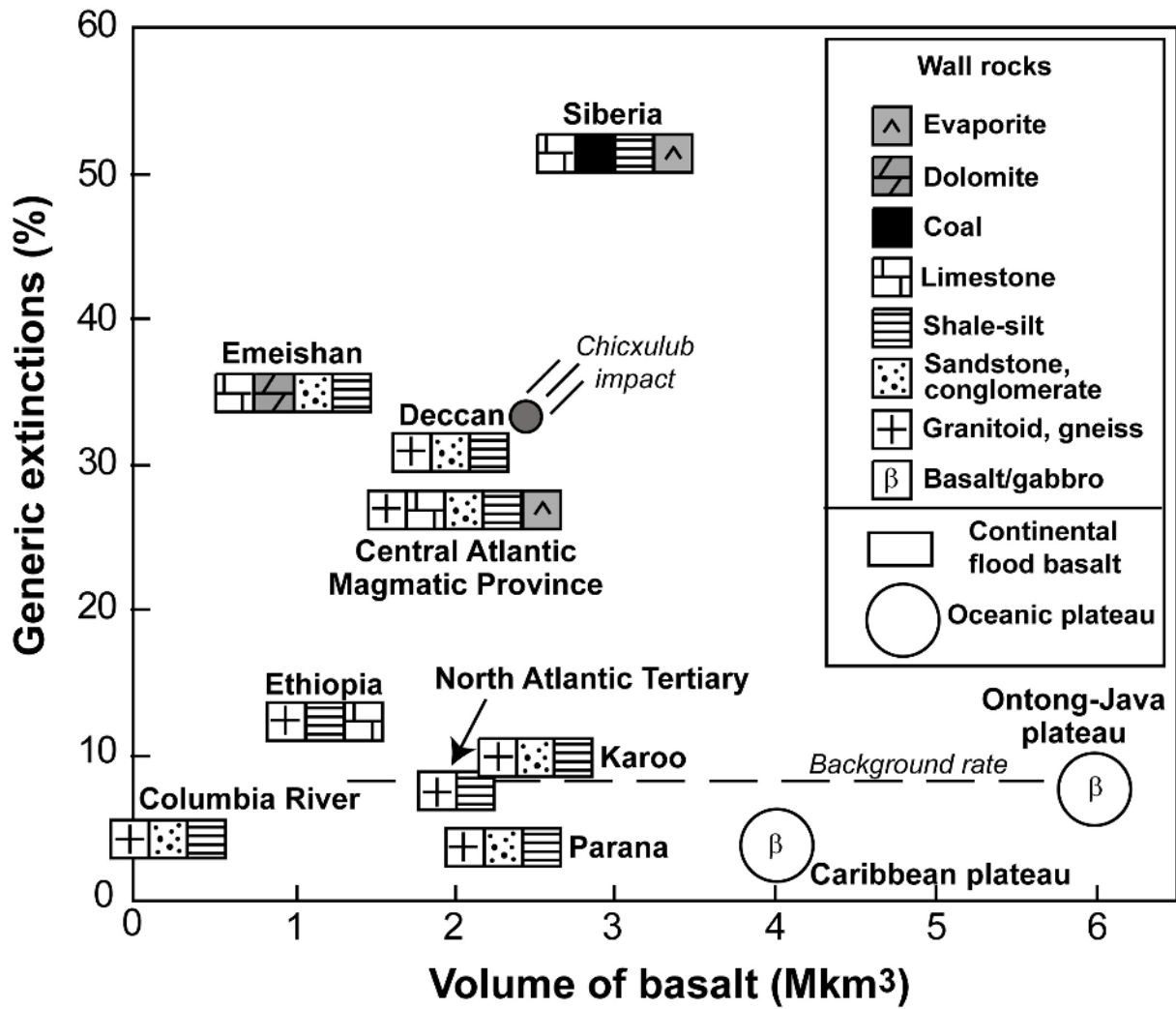
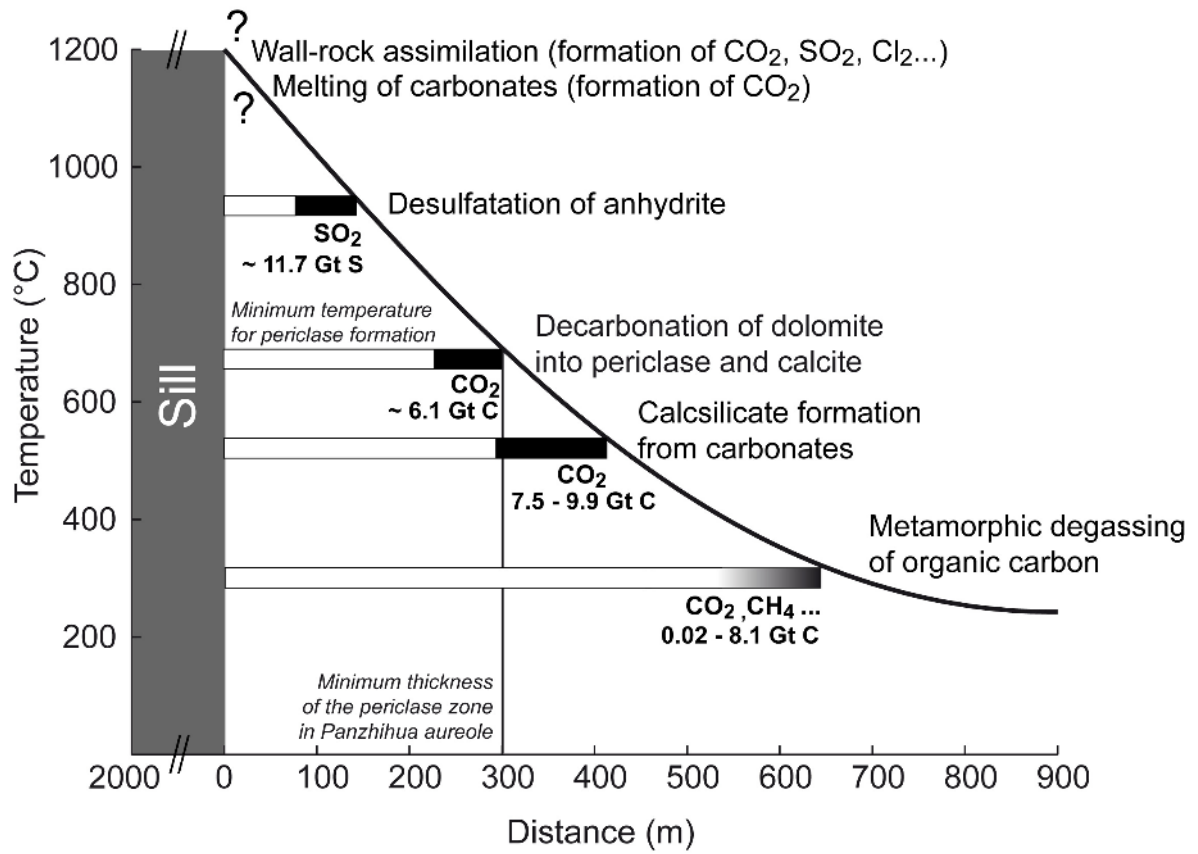


Fig.2



362
363
364 |

365 **Supplementary material 1: Degassing during contact metamorphism as**
366 **an explanation of the negative carbon isotope excursion associated with**
367 **the emplacement of the Emeishan LIP**
368

369 Our measurements of the $\delta^{13}\text{C}$ of dolostones from the Sinian formation range from +4.7
370 to -1.1, values which are consistent with Jacobsen and Kaufman's (1998) estimate of
371 $\delta^{13}\text{C}$ in Neoproterozoic seawater (+4 to -4 ‰, with most of the data between +2 and -2
372 ‰). If we assume that (1) end-Guadalupian seawater contained ~40000 Gt C with $\delta^{13}\text{C}$
373 = +5 ‰ (Berner, 2005), (2) end-Guadalupian atmosphere contained ~2850 Gt C
374 (Rothman 2002) with $\delta^{13}\text{C}$ = -2 ‰ (7 ‰ more negative than seawater (Mora et al.
375 1996)), then the average $\delta^{13}\text{C}$ of the ocean-atmosphere system was +4.5.

376 After the addition of 16800 Gt of magmatic CO_2 (4580 Gt C with $\delta^{13}\text{C}$ = -6),
377 62500 Gt of CO_2 from destabilized Sinian dolostone (17000 Gt C with $\delta^{13}\text{C}$ = 0) and
378 potentially 84000 Gt CO_2 from the metamorphism of organic carbon (=22900 Gt C
379 with $\delta^{13}\text{C}$ ~ -22), the bulk composition of the ocean-atmosphere system is changed to
380 between $\delta^{13}\text{C}$ = +2.6 ‰ (if no organic contribution) and -3.9 (if 22900 Gt C from the
381 metamorphism of organic carbon was added with $\delta^{13}\text{C}$ ~ -22). If we then assume that
382 ocean-atmosphere equilibrium is rapid (flux ~90 Gt/y as current estimation) and the
383 difference between the carbon isotope compositions of ocean and atmosphere is fixed at
384 the timescales we consider ($\delta^{13}\text{C}_{\text{atm}} = \delta^{13}\text{C}_{\text{ocean}} - 7$ ‰), as supposed by Mora (1996) and
385 Beerling et al. (2002), then the effect of emplacement of the Emeishan LIP in the Sinian
386 Basin is a negative carbon excursion for the ocean-atmosphere system from an average
387 of $\delta^{13}\text{C}$ = -2 before the degassing to an average of $\delta^{13}\text{C}$ = -4.4 to -10.9 after degassing.
388

389 References cited

- 390 Beerling, D.J., Lake, J.A., Berner, R.A., Hickey, L.J., Taylor D.W., and Royer D.L.,
391 2002, Carbon isotope evidence implying high O_2/CO_2 ratios in the Permo-
392 Carboniferous atmosphere. *Geochimica et Cosmochimica Acta*, v. 66, p. 3757-
393 3767, doi: 10.1016/S0016-7037(02)00901-8.
- 394 Berner, R.A., 2005, The carbon and sulphur cycles and atmospheric oxygen from
395 middle Permian to middle Triassic: *Geochimica et Cosmochimica Acta*, v. 69,p.
396 3211-3217, doi: 10.1016/j.gca.2005.03.021.
- 397 Jacobsen, S.B., and Kaufman, A.J., 1999, The Sr, C and O isotopic evolution of
398 Neoproterozoic seawater: *Chemical Geology*, v. 161, p. 37-57, doi:
399 10.1016/S0009-2541(99)00080-7.
- 400 Mora, C.I., Driese, S.G., and Colarusso, L.A., 1996, Middle to Late Paleozoic
401 Atmospheric CO_2 Levels from Soil Carbonate and Organic Matter: *Science*, v.
402 271, p. 1105-1107, doi: 10.1126/science.271.5252.1105.

403

404 |

405

406 **Supplementary material 2: An overview of reactions in a metamorphic**
407 **aureole in a sedimentary basin**

408 The amount of gas released during metamorphism depends on the type of sediment and
409 its chemical composition, and on the conditions (P,T, Xfluid) of metamorphism.

- 410 • At the highest temperatures, calcite melts incongruently to CaO and CO₂. Solid or
411 liquid calcite is assimilated into the magma where it reacts to Ca which is absorbed
412 in the magma or overlying rocks and CO₂, which degasses.
- 413 • Thermal decomposition of pure anhydrite ($\text{CaSO}_4 = \text{CaO} + \text{SO}_2 + \frac{1}{2} \text{O}_2$) begins at
414 1100°C and reacts readily only at temperatures around 1400 °C. Impure anhydrite
415 containing clay, graphite or carbon monoxide reacts at temperatures well below
416 1000°C ($2\text{CaSO}_4 + \text{C} = 2\text{CaO} + \text{CO}_2 + 2\text{SO}_2$ and $\text{CaSO}_4 + \text{CO} = \text{CaO} + \text{CO}_2 +$
417 SO_2). Kuusik et al. (1985) report thermal decomposition of anhydrite in CO/N
418 mixtures at 900 °C. Impurities such as SiO₂ lower the decomposition temperatures
419 by up to 100 °C. West and Sutton (1954) report decomposition of anhydrite with
420 20% added carbon at 615°C in a nitrogen atmosphere.
- 421 • Thermal decomposition of pure limestone ($\text{CaCO}_3 = \text{CaO} + \text{CO}_2$) strongly depends
422 on the water content. In the absence of water, decomposition starts only at high
423 temperature, around 1200°C; when aqueous fluid is present, the temperature is
424 lower (~700°C).
- 425 • Dolomite reacts to calcite, periclase and CO₂ ($\text{CaMg}(\text{CO}_3)_2 = \text{CaCO}_3 + \text{MgO} +$
426 CO_2) at 700°C. In the presence of aqueous fluid the temperature decreases to below
427 ~450°C
- 428 • Calc-silicates containing forsterite and diopside form from impure limestones and
429 marls. These reactions release considerable CO₂ and proceed at relatively low
430 temperatures, between 450 and 500°C.
- 431 • Organic matter in carbonates or shales releases CH₄ and/or CO₂. Cracking of
432 hydrocarbons starts at ~100°C and reaches a maximum around 550 °C.
- 433 • Other gases are released from specific sediment types. Salts break down to
434 halogens; pyrite in sulfide-rich shales oxidises or breaks down to Fe-oxide releasing
435 sulfur oxides; coal burns to release CO₂.

436 The reactions within an aureole thus release a series of greenhouse or toxic gases,
437 including CO₂, SO₂, CH₄, and halogens, as summarized in Figure 2.

438

439 **References cited**

440 Kuusik, R., Saikkonen, P., and Niinisto, L., 1985, Thermal decomposition of calcium
441 sulfate in carbon monoxide: Journal Thermal Analysis and Calorimetry, v. 30,
442 p. 187-193.

443

444

445

446